Available online at www.sciencedirect.com
SCIENCE DIRECT
Journal of Power Sources 158 (2006) 129–136
JOURNAL OF POWER SOURCES
www.elsevier.com/locate/jpowsour

Characterization of a high performing passive direct formic acid fuel cell

S. Ha [1], Z. Dunbar, R.I. Masel *

University of Illinois, Department of Chemical and Biomolecular Engineering, 600 S Mathews, Urbana, IL 61801, USA

Received 23 July 2005; accepted 27 September 2005
Available online 28 December 2005

Abstract

Small fuel cells are considered likely replacements for batteries in portable power applications. In this paper, the performance of a passive air breathing direct formic acid fuel cell (DFAFC) at room temperature is reported. The passive fuel cell, with a palladium anode catalyst, produces an excellent cell performance at 30 °C. It produced a high open cell potential of 0.9 V with ambient air. It produced current densities of 139 and 336 mA cm^{-2} at 0.72 and 0.53 V, respectively. Its maximum power density was 177 mW cm^{-2} at 0.53 V. Our passive air breathing fuel cell runs successfully with formic acid concentration up to 10 and 12 M with little degradation in performance. In this paper, its constant voltage test at 0.72 V is also demonstrated using 10 M formic acid. Additionally, a reference electrode was used to determine distinct anode and cathode electrode performances for our passive air breathing DFAFC.

Keywords: Direct formic acid fuel cell; Portable power; Reference electrode

1. Introduction

Recently, there has been considerable interest in the use of miniature fuel cells as replacements for batteries in portable electronics. The advantages of using miniature fuel cells over conventional batteries are that the miniature fuel cells have a much higher stored energy density, and the ability to be immediately recharged by replacing the fuel cartridge [1]. Most investigators are exploring direct methanol fuel cells (DMFCs) for this purpose [2,3], but our previous paper showed that direct formic acid fuel cells (DFAFCs) are quite interesting for portable power applications [4–8].

Formic acid is a liquid, but unlike methanol it has a low crossover through the Nafion® membrane and a high kinetic activity. These unique characteristics of formic acid allow to operate DFAFCs at higher voltages than DMFCs. Methanol has the higher theoretical energy density than formic acid. However, because fuel cells run more efficiently at higher voltages, in practice DFAFCs have about the same energy density as DMFCs. Furthermore, DFAFCs have about a factor of three to six higher power density than DMFCs and can operate well at room temperatures [4–8]. Thus, DFAFCs have advantages over DMFCs.

In the previous study, the passive air breathing DFAFC with PtRu black anode catalyst produced a maximum power density of 33 mW cm^{-2} [6]. This power output is very promising and far better than that of most reported passive DMFCs, but it still needs a significant performance improvement in order to compete with the conventional batteries. In order to bring such improvement, we need to develop more active catalysts for oxidizing formic acid. This catalytic improvement would increase cell efficiency and power density while reducing overall precious metal loadings.

Recently, noble Pd catalysts were found which produced unusually high performances in active DFAFCs. Until now, Pd catalyst has never been tested for passive DFAFCs. Like active DFAFCs, we expect to find a similar significant performance enhancement in passive DFAFCs with Pd black catalyst. In this study, we characterize the performance of the passive air breathing DFAFC with Pd black catalyst. To determine its distinct anode and cathode electrode performances, a reference electrode is used. The performance of the passive DFAFC is also compared to that of the active DFAFC.

* Corresponding author. Tel.: +1 217 333 6841; fax: +1 217 333 5052.
E-mail address: r-masel@uiuc.edu (R.I. Masel).
[1] Present address: Chemical Engineering Dept., Washington State University, Dana 118, Pullman, WA 99164-2710, USA.

0378-7753/$ – see front matter © 2005 Elsevier B.V. All rights reserved.
doi:10.1016/j.jpowsour.2005.09.048

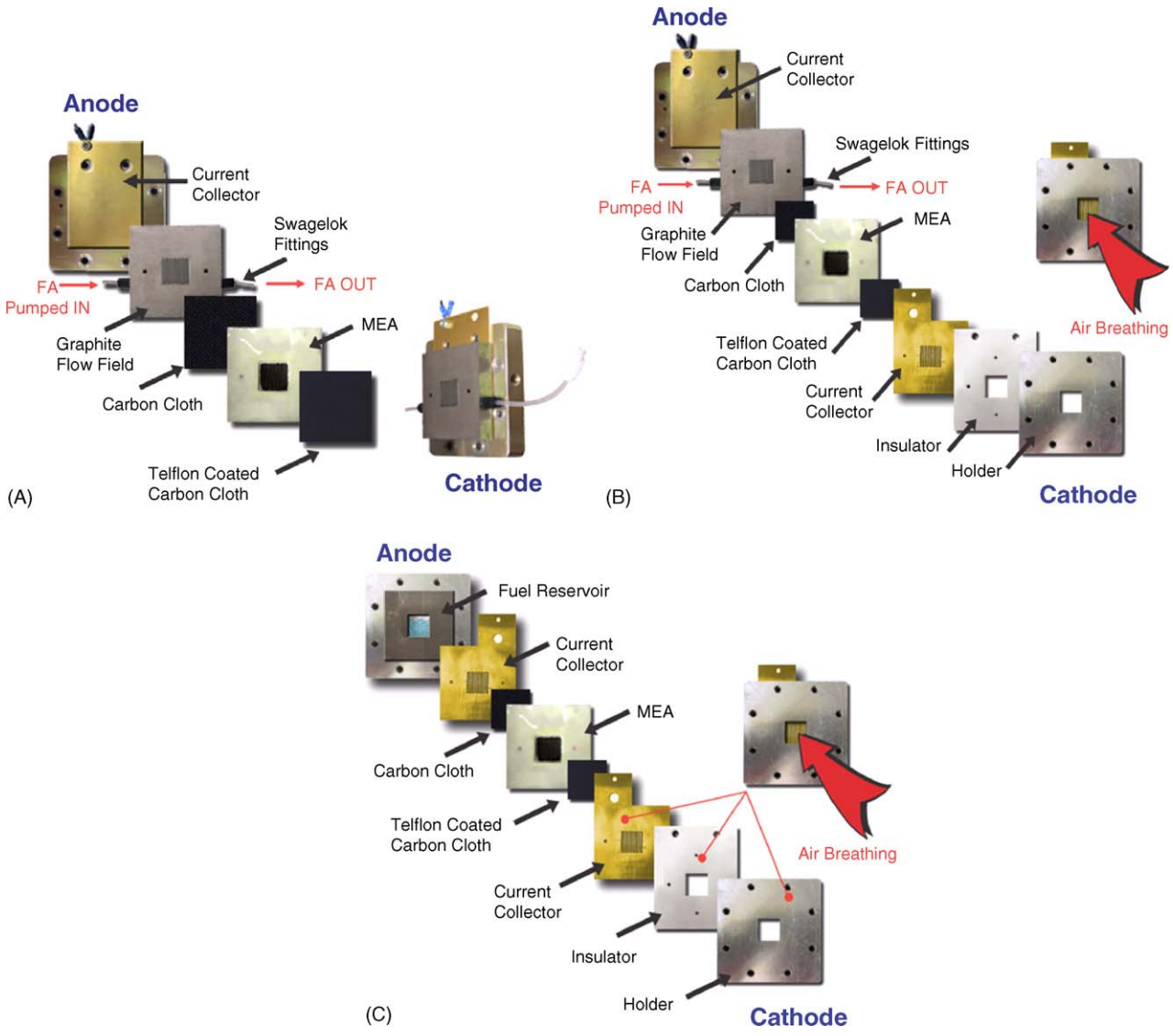

Fig. 1. Diagrams of (A) the active, (B) the active air breathing, and (C) the passive air breathing DFAFCs.

2. Experimental

The membrane electrode assemblies (MEA) were fabricated in house using a 'direct paint' technique as it is described elsewhere [4–6,8]. The active area is 4 cm^2. The 'catalyst inks' were prepared by dispersing the catalyst powders into appropriate amounts of Millipore water and 5% recast Nafion® solution (1100EW, Solution Technology, Inc.). Then both the anode and the cathode 'catalyst inks' were directly painted onto either side of the Nafion® 115 membrane. A commercially available platinum black (HiSPEC™ 1000 from Johnson Matthey) was used for the cathode catalyst layer at a loading of 8 mg cm^{-2}. Pd black (High Surface Area from Sigma–Aldrich) was used for the anode catalyst layer at a loading of 8 mg cm^{-2}. The final catalyst layers contained 15% Nafion® by weight.

As Fig. 1 shows, three different types of DFAFC were used in this study: active DFAFC, active air breathing DFAFC (air breathing DFAFC), and passive air breathing DFAFC (passive DFAFC). In the active DFAFC, both formic acid and air were supplied to the catalyst layers through flow fields using a liquid syringe pump and a compressed gas cylinder. For the air breathing DFAFC, the cathode flow field was removed from the active DFAFC and the cathode was exposed to the ambient air. For the passive DFAFC, both the anode and cathode flow fields were removed from the active DFAFC and a fuel reservoir was placed at the anode. Formic acid was delivered from the fuel reservoir to the anode catalyst layer by a simple diffusion and capillary action in the passive DFAFC. Both a heating cartridge and heating tape were used to maintain the operating cell temperature at 30 °C. Formic acid from Fluka® was diluted with the Millipore water to give a final concentration ranging from 3 to 15 M. The membrane was used without any prior conditioning.

Both cell polarization curves and constant voltage test were acquired using a fuel cell testing station (Fuel Cell Technologies, Inc.). An Ag/AgCl reference electrode from Fisher® mounted in the fuel reservoir in Fig. 1(B) was used to measure the anode

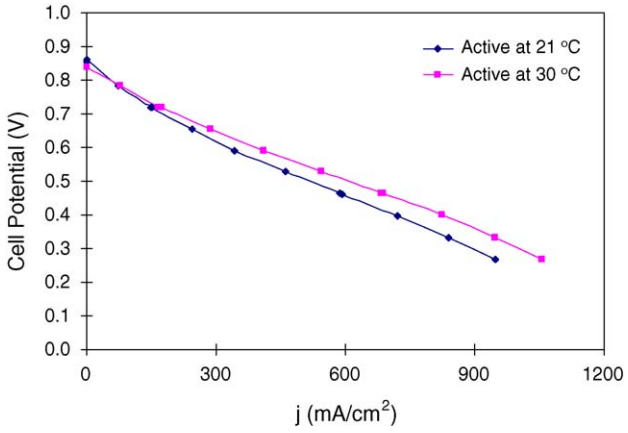

Fig. 2. Fuel cell polarization plots of the active DFAFC at 22 and 30 °C. Ten molal formic acid was used at a flow rate of 1 ml min^{-1}. The dry air was supplied to the cathode at a flow rate of 390 sccm without backpressure. PdBl and PtBl were used for the anode and cathode electrode, respectively.

potential for the passive air breathing DFAFC. We also calculated a cathode potential via

$$(\text{cathode potential}) = (\text{anode potential}) + (\text{cell potential}) + IR$$

where I equals the current in mA cm^{-2} and R is the measured high frequency resistance.

3. Results

Fig. 2 illustrates the current voltage characteristics of the active DFAFC at two different operating temperatures using 10 M formic acid. Note that the currents are normalized by the geometrical surface area of the MEA (4 cm^2) in Fig. 2. Fig. 2 shows that the active DFAFC produces an excellent current density output at moderate operating temperatures. For an example, the active DFAFC at 30 °C produces a current density of 174 and 683 mA cm^{-2} at 0.72 and 0.46 V, respectively. According to Fig. 2, the active DFAFC generally produces a better performance at 30 °C than 21 °C. For an example, the active DFAFC at 30 °C provides 40 mV advantages over the active DFAFC at 21 °C at 460 mA cm^{-2}.

Fig. 3(A) shows comparison current voltage characteristic plots between three different types of DFAFC: the active DFAFC, the air breathing DFAFC, and the passive DFAFC. According to Fig. 3(A), there is relatively little difference in the cell performance between them at the high cell potential range (between 0.9 and 0.7 V). However, the current voltage characteristic plot of the air breathing DFAFC starts to deviate from that of the active DFAFC at 0.7 V in Fig. 3(A). According to Fig. 3(A), the current density output increases almost linearly from 174 to 1057 mA cm^{-2} for the active DFAFC as the cell potential decreases from 0.70 to 0.26 V. On the other hand, the air breathing DFAFC shows a much smaller current density increase for the same potential drop. Especially, the air breathing DFAFC shows a rapid falling in its current voltage characteristic plot at the cell potential of 0.52 V and below in Fig. 3(A). Hence, as the cell potential decreases from 0.70 V and below, the performance difference between the active and

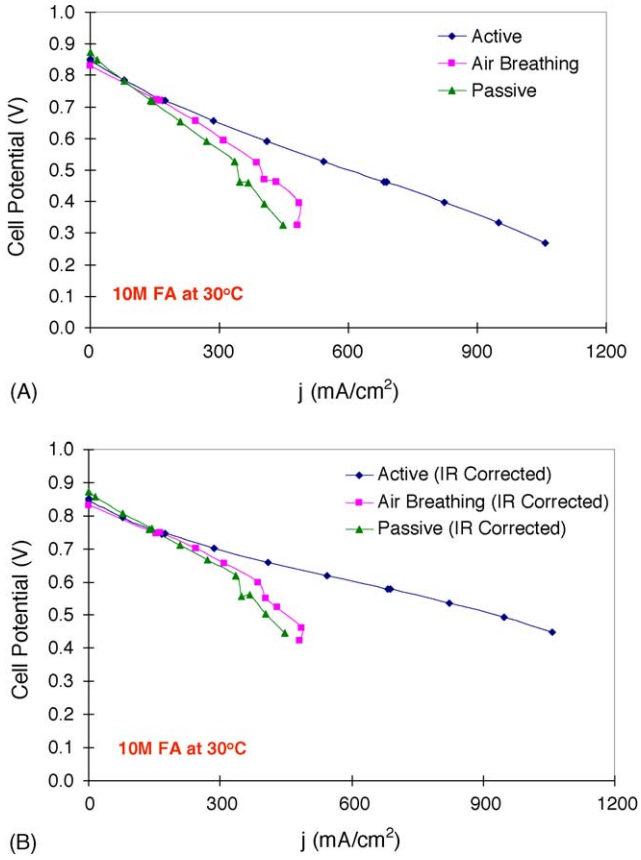

Fig. 3. (A) Actual fuel cell polarization plots and (B) *I–R* corrected fuel cell polarization plots of the active, the active air breathing, and the passive air breathing DFAFCs with 10 M formic acid at 30 °C. For the active DFAFC, formic acid and dry air were supplied to the anode and the cathode at a rate of 1 ml min^{-1} and 390 sccm without backpressure, respectively. For the active air breathing DFAFC, only formic acid was supplied to the anode at a rate of 1 ml min^{-1} while the cathode was breathing ambient air. For the passive air breathing DFAFC, there was no active pumping of the fuel at the anode and the formic acid was delivered passively from the fuel reservoir to the anode. PdBl and PtBl were used for the anode and cathode electrode, respectively.

the air breathing DFAFCs increases significantly. According to Fig. 3(A), the passive DFAFC follows a similar trend as the air breathing DFAFC except it shows even lower performance at 0.7 V and below. In Fig. 3(B), *I–R* drops are corrected from the current voltage characteristic plots of Fig. 3(A). By doing so, Fig. 3(B) allows one to compare the cell performance in an absent of cell resistances. According to Fig. 3(B), all three types of DFAFC follow similar current voltage characteristic trends as those in Fig. 3(A). For an example, at the high cell potentials, all three types of DFAFC show similar cell performances. However, at the lower cell potentials, the performances of both the air breathing and the passive DFAFCs start to deviate from that of the active cell and show much smaller performances than the active cell.

Fig. 4 plots the anode, the cathode, and the *I–R* corrected cell polarization curves of the passive air breathing DFAFC using 10 M formic acid at 30 °C. The anode and the cathode polarization plots differ from the cell polarization plot, in that their potentials are measured versus a silver/silver chloride reference electrode and converted to RHE. This allows

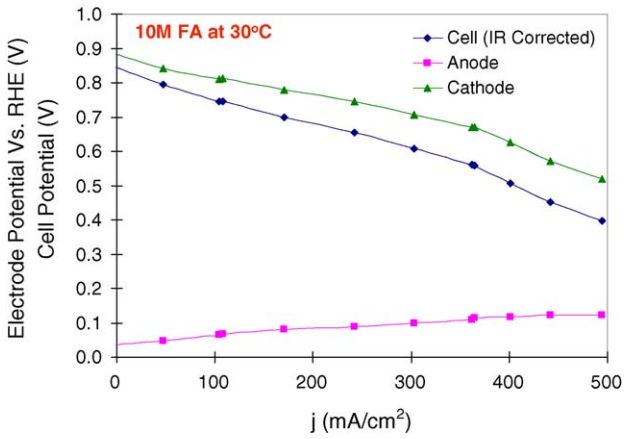

Fig. 4. The anode, the cathode, and the *I–R* corrected cell polarization curves of the passive air breathing DFAFC using 10 M formic acid at 30 °C. Formic acid was delivered passively from the fuel reservoir to the anode while the cathode was breathing ambient air. The Ag/AgCl reference electrode was used to measure the distinct anode and the cathode potential during acquisition of the cell polarization. PdBl and PtBl were used for the anode and cathode electrode, respectively.

one to facilitate the quantitative analysis of the isolated anode and cathode performances. According to Fig. 4, the OCP of the anode electrode is 37 mV versus RHE. Fig. 4 shows that the anode potential increases by 90 mV from its OCP as the current density increases from 0 to 500 mA cm^{-2}. This potential change of the electrode from its OCP is known as the over-potential. According to Fig. 4, the most of the anode over-potential occurs between 0 and 400 mA cm^{-2}. As the current density increases continuously beyond 400 mA cm^{-2}, Fig. 4 indicates that the anode over-potential is almost constant. According to Fig. 4, the OCP of the cathode electrode is 0.882 mV versus RHE. Contrast to the anode electrode, the cathode electrode of the passive DFAFC shows a significant over-potential as the current density increases in Fig. 4. For an example, Fig. 4 shows that the cathode over-potential increases by more than 360 mV as the current density increases from 0 to 500 mA cm^{-2}. According to Fig. 4, the cathode over-potential increases in a much faster rate at the high current density region than at the low current density region. For an example, as the current density increases from 0 to 365 mA cm^{-2}, the cathode over-potential increases at a rate of 0.58 mV per 1 mA cm^{-2} in Fig. 4. As the current density increases continuously beyond 365 mA cm^{-2}, the cathode over-potential increases at a rate of 1.17 mV per 1 mA cm^{-2}. According to Fig. 4, the *I–R* corrected cell polarization plot shows a similar voltage-current characteristic as the cathode polarization plot.

Fig. 5(A) shows the effect of varying the formic acid concentration from 3 to 15 M on the cell polarization curve profile of the passive air breathing DFAFC at 30 °C. The largest current densities over the entire cell potential range that we studied are observed using formic acid concentration between 8 and 10 M. As the concentration of formic acid is increased from 3 to 10 M, the current density generated by the passive DFAFC also increases. However, as the concentration of formic acid is continuously increased from 10 to 15 M, the current density starts to decrease.

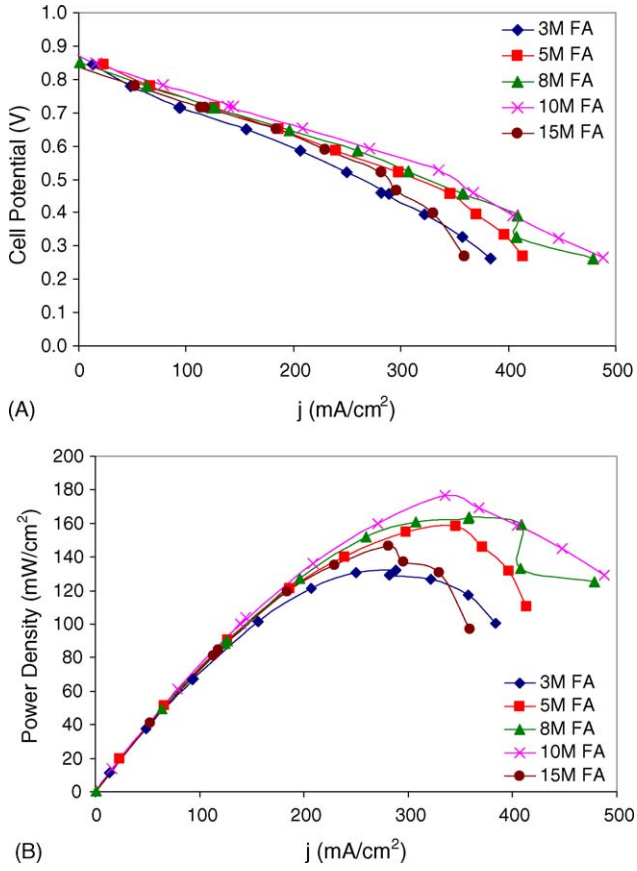

Fig. 5. Passive air breathing DFAFC vs. the formic acid concentration at 30 °C: (A) cell potential and (B) power density curves. Formic acid was delivered passively from the fuel reservoir to the anode while the cathode was breathing ambient air. PdBl and PtBl were used for the anode and cathode electrode, respectively.

In Fig. 5(B), the results from Fig. 5(A) are plotted in terms of power density for the different formic acid concentration. In general, a power density output increases as the formic acid concentration increases from 3 to 10 M. From Fig. 5(B), the passive DFAFC with 10 M formic acid can produce a maximum power density of 177 mW cm^{-2} at 0.53 V. As the formic acid concentration increases continuously from 10 to 15 M, overall power density output decreases. However, the passive DFAFC with 15 M formic acid still produces a significant power density of 147 mW cm^{-2} at 0.53 V, which is about 17% performance reduction from the cell with 10 M formic acid.

In Fig. 6, the power density of the passive DFAFC at 0.40 V is plotted as a function of the formic acid concentration at 30 °C. The power density is attained from Fig. 5(A). The passive DFAFC with 10 M formic acid generates the largest power density of 160 mW cm^{-2} at 0.40 V and 30 °C. As the concentration of formic acid is increased from 10 to 15 M, the cell performance is gradually decreased.

Fig. 7 plots the anode polarization curves of the passive DFAFC for different formic acid concentrations ranging from 10 to 15 M at 30 °C. In general, Fig. 7 shows that the anode potential

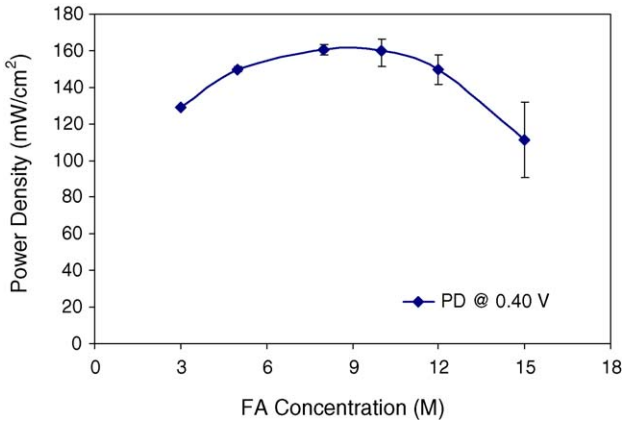

Fig. 6. Plot of formic acid feed concentration vs. power density at 0.40 V cell potential for passive air breathing DFAFC. The cell temperature was 30 °C. Different formic acid concentrations (3, 5, 8, 10, and 15 M) were delivered passively from the fuel reservoir to the anode while the cathode was breathing ambient air. PdBl and PtBl were used for the anode and cathode electrode, respectively.

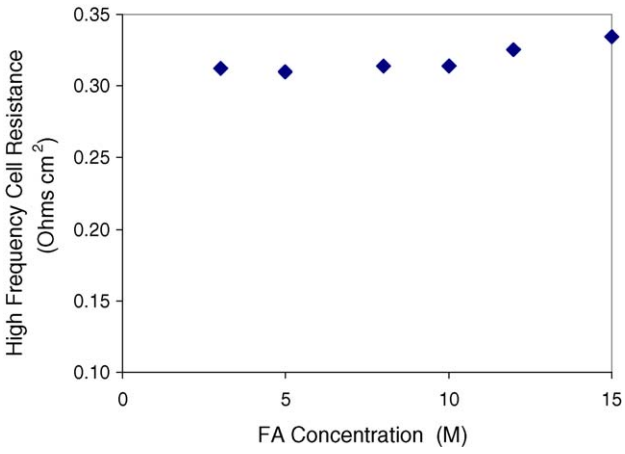

Fig. 8. Influence of formic acid concentration vs. cell resistance for passive air breathing DFAFC. The cell temperature was 30 °C. The difference concentrations of formic acid were delivered passively from the fuel reservoir to the anode. The cathode was breathing ambient air. PdBl and PtBl were used for the anode and cathode electrode, respectively.

increases over the entire current density range as the concentration of formic acid is increased from 10 to 15 M. For example, the anode potential of the passive DFAFC at 156 mA cm^{-2} is 90, 96, and 111 mV versus RHE for 10, 12, and 15 M formic acid, respectively, in Fig. 7. During the cell polarization curve acquisition, the high frequency cell resistance is also measured. Fig. 8 highlights the effect of the formic acid concentration on the high frequency cell resistance. The cell resistance is independent of formic acid concentration between 3 and 10 M. However, it slowly increases from 0.314 to 0.334 Ω cm^2 as the formic acid concentration is increased from 10 to 15 M.

Fig. 9 provides a constant voltage test of the passive DFAFC at 0.72 V and 30 °C using 10 M formic acid. Fig. 9 shows that the passive DFAFC initially generates approximately 125 mA cm^{-2} at 0.72 V. However, the current density decreases as the cell operation time increases in Fig. 9. According to Fig. 9, its initial current density drop is sharp, followed by a slower decay. For an example, the current density drops by more than 25 mA cm^{-2} for the first 0.1 h (6 min), while it drops by less than 40 mA cm^{-2} for the following 1.4 h (84 min). In longer runs, we found that there continues to be a slow decay in current density, followed by a rapid decay when formic acid is depleted in the fuel reservoir.

Fig. 10 provides a constant current test of the passive DFAFC at 100 mA cm^{-2} and 30 °C using 10 M formic acid. In Fig. 10, the distinct anode, cathode, and cell potentials are plotted versus the operation time using the reference electrode. According to Fig. 10, initial anode and cathode potentials are 80 and 793 mV versus RHE, respectively. As the cell operation time increases for the first 3.3 h (200 min), the anode over-potential increases by less than 120 mV. However, as the passive DFAFC runs continuously beyond 3.3 h, the anode over-potential shows a rapid increase. According to Fig. 10, the anode over-potential increases up to 594 mV after operating the cell for 4.4 h.

Fig. 10 shows that the cell potential follows a similar trend as the anode potential over the operation time. For an example, like the anode potential, the cell potential deviates from its ini-

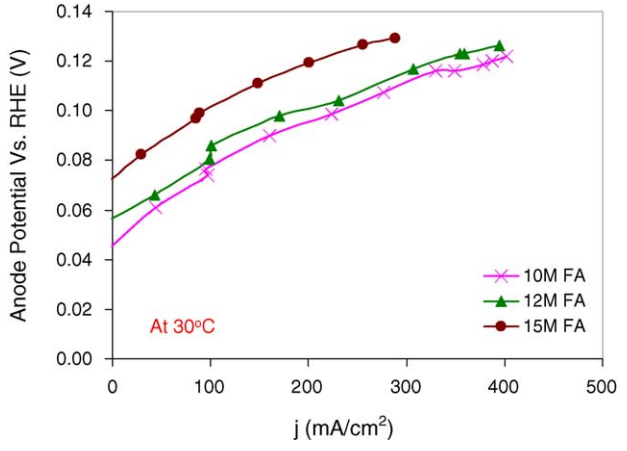

Fig. 7. Anode polarization curves of passive air breathing DFAFC at 30 °C with different formic acid concentrations (10, 12, and 15 M) using the Ag/AgCl reference electrode. There was no active pumping of the fuel at the anode and the formic acid was delivered passively from the fuel reservoir to the anode. The cathode was breathing ambient air. PdBl and PtBl were used for the anode and cathode electrode, respectively.

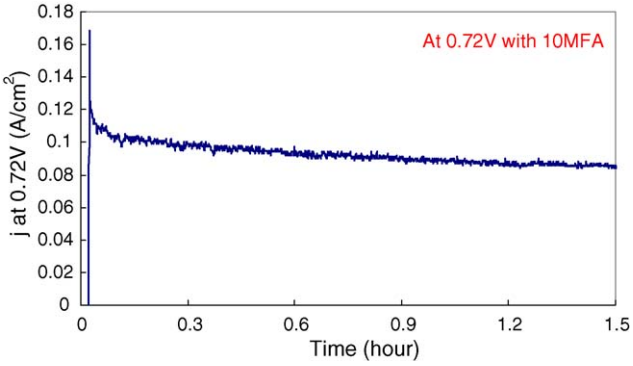

Fig. 9. Plot of constant cell potential test at 0.72 V for passive air breathing DFAFC. Ten molal formic acid was delivered passively from the fuel reservoir to the anode. The cathode was breathing ambient air. PdBl and PtBl were used for the anode and cathode electrode, respectively.

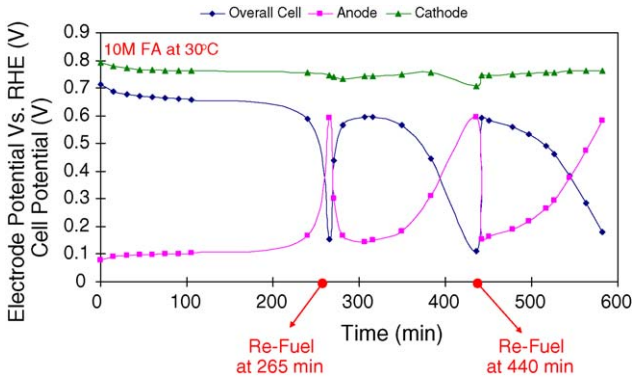

Fig. 10. Plot of constant current density test at 100 mA cm^{-2} for passive air breathing DFAFC. The anode, the cathode, and overall cell potentials were measured simultaneously using the Ag/AgCl reference electrode at 30 °C. Ten molal formic acid was delivered passively from the fuel reservoir to the anode. The cathode was breathing ambient air. PdBl and PtBl were used for the anode and cathode electrode, respectively.

tial value rapidly only after the cell runs for more than 3.3 h in Fig. 10. In Fig. 10, the anode fuel reservoir is refueled with a fresh 10 M formic acid at 4.4 and 7.3 h (265 and 440 min) of the operation time. As soon as the fresh 10 M formic acid is supplied to the anode fuel reservoir in each time, most of the anode over-potential disappears and the cell potential restores most of its initial value in Fig. 10. However, after refueling the cell, the anode over-potential starts to increase again, while the cell potential starts to decrease gradually as the cell continues to run in Fig. 10. According to Fig. 10, the cathode potential remains relatively constant over 10 h of the operation time.

In this study, we also used an empirical model to understand the performance difference that we observed between the passive and active DFAFCs. In general, the cell potential drops as the current density increases because of fuel cell irreversibilities. There are four major irreversibilities: (1) activation losses, (2) fuel crossover, (3) ohmic losses, and (4) mass transport losses. We can combine all these irreversibilities and arrive at the following equation for the operating potential of the fuel cell as a function of current density [9]:

$$V = E - (i + i_n)R - A_{(a)} \ln\left(\frac{i + i_n}{i_{o(a)}}\right) - A_{(c)} \ln\left(\frac{i + i_n}{i_{o(c)}}\right) + B_{(a)} \ln\left(1 - \frac{(i + i_n)}{i_{l(a)}}\right) + B_{(c)} \ln\left(1 - \frac{(i + i_n)}{i_{l(c)}}\right) \quad (1)$$

In Eq. (1), E is the reversible open cell voltage, i_n the fuel crossover equivalent current density, R the area specific resistance, $A_{(a)}$ and $A_{(c)}$ the slop of the Tafel line for the anode and the cathode, respectively, $i_{o(a)}$ and $i_{o(c)}$ the exchange current density at the anode and the cathode, respectively, $B_{(a)}$ and $B_{(c)}$ the mass transfer parameter for the anode and the cathode, respectively, and $i_{l(a)}$ and $i_{l(c)}$ are the limiting current density at the anode and the cathode, respectively. Eq. (1) is fitted using EXCEL spreadsheet to the cell polarization plots of the active and the passive DFAFCs in Fig. 3(A). Fig. 11 shows how our model equation fits well with the actual experimental data. Table 1 summarizes all the model results in this study.

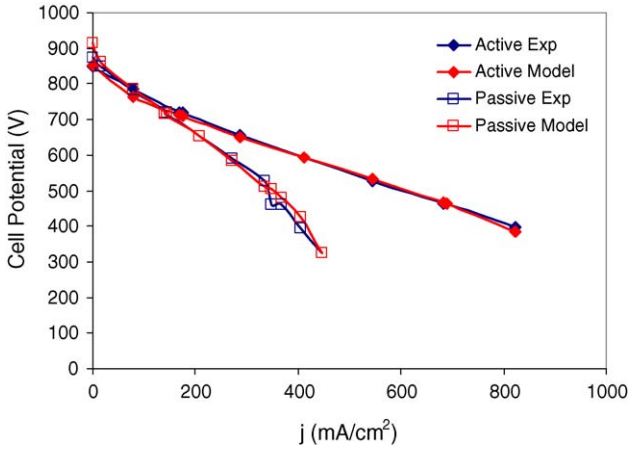

Fig. 11. The empirical equation relating the cell potential as a function of irreversibilities was used to fit the experimental cell polarization plots for both the active and the passive air breathing DFAFCs at 30 °C. PdBl and PtBl were used for the anode and cathode electrode, respectively.

Table 1
Summary of results from an empirical modeling on both the active and the passive DFAFC

Active DFAFC		Passive DFAFC	
E, emf (mV)	1450	E, emf (mV)	1450
i_n (mA cm^{-2})	146	i_n (mA cm^{-2})	89
$A_{(a)}$ (mV)	28	$A_{(a)}$ (mV)	26
$i_{o(a)}$ (mA cm^{-2})	25	$i_{o(a)}$ (mA cm^{-2})	38
$B_{(a)}$ (mV)	60	$B_{(a)}$ (mV)	118
$i_{l(a)}$ (mA cm^{-2})	1208	$i_{l(a)}$ (mA cm^{-2})	880
$A_{(c)}$ (mV)	65	$A_{(c)}$ (mV)	62
$i_{o(c)}$ (mA cm^{-2})	0.039	$i_{o(c)}$ (mA cm^{-2})	0.04
$B_{(c)}$ (mV)	30	$B_{(c)}$ (mV)	59
$i_{l(c)}$ (mA cm^{-2})	1204	$i_{l(c)}$ (mA cm^{-2})	557

4. Discussion

The results here provide further evidence that DFAFCs are quite attractive for portable power applications. The result in Fig. 5 shows that our passive DFAFC with the Pd black catalyst produces 177 mW cm^{-2} at 0.53 V using 10 M formic acid at ambient temperature. By comparison our previous passive DFAFC with the PtRu Black catalyst produces only 3 mW cm^{-2} at 0.53 V under the similar conditions. Clearly, our passive DFAFC shows a significant performance enhancement by increasing the anode catalytic activity with the Pd black catalyst.

Liu et al. [10] report that his passive DMFC produced a maximum power density of about 20 mW cm^{-2} at 0.15 V under conditions similar to those reported here. Kim et al. [11] report that their passive DMFC produced a maximum power density of 40 mW cm^{-2} at 0.3 V. Clearly, our passive DFAFC shows a superior advantage over other passive DMFCs in terms of power output. Our DFAFC also compares well with DMFC in terms of fuel energy density. According to Figs. 5 and 6, the passive DFAFC runs successfully with 10 M formic acid solution and generates 140 mA cm^{-2} at 0.72 V. By comparison, the best performing passive DMFC generates about 140 mA cm^{-2}

at 0.28 V with 4 M methanol solution [11]. If neat formic acid is fed into a fuel cell operating at 0.72 V, the fuel cell will generate 1024 Wh l^{-1} of fuel ignoring parasitic losses. By comparison if neat methanol is fed into a fuel cell operating at 0.28 V, the methanol fuel cell will generate 1110 Wh l^{-1} ignoring parasitic losses. Thus, DFAFC and DMFCs have very similar net energy densities under real operating conditions but the formic acid fuel cells produce much more power.

Finally, OCP of the fuel cell is quite reasonable. The passive cell in Fig. 5(A) shows an OCP of 873 mV with 10 M formic acid. By comparison Liu et al. report an OCP of 495 mV for a passive DMFC with only 5 M methanol. Overall, the passive DFAFC shows an excellent performance compared to the passive DMFC.

There are some surprises in the data too. First, there is a significant difference of the cell performance between the active air delivery system (in active DFAFC) and the passive air delivery system (in air breathing DFAFC) in Fig. 3. Yet, according to Fig. 3, the cell performance between the active fuel delivery system (in air breathing DFAFC) and the passive fuel delivery system (in passive DFAFC) changes less significantly. During the cell polarization test, the cathode potential decreases rapidly as the cell current density increases, while the anode potential does not change much from its OCP in Fig. 4. These results from Figs. 3 and 4 indicate that the performance of the passive DFAFC with 10 M formic acid is mostly limited by its low cathode performance. This low cathode performance of the passive cell occurs mainly by a poor mass transport of the oxygen (or the oxygen from air) to its cathode catalyst layer. This view agrees well with the results from our empirical model (Fig. 11 and Table 1). According to our model results, most of the kinetic parameters (anode Tafel slop, cathode Tafel slop, and cathode exchange current density) and the anode limiting current density do not change much between the active and passive DFAFCs. However, the cathode limiting current density decreases significantly from the active to the passive DFAFCs. The limiting current density is a good indictor of showing how severely the cell is limited by the mass transport process. Hence, our model results clearly indicate that the performance of the passive cell is limited mainly by the poor mass transport of the cathode.

Figs. 5 and 6 show that the optimal formic acid concentration at 30 °C is about 10 M for the Pd black based passive DFAFC. The following trends are found in Figs. 5 and 6. As formic acid concentration is increased from 3 to 15 M, both the cell polarization current densities and the power densities are increased initially up to 10 M. However, they decrease rapidly as formic acid concentration is increased continuously from 10 to 15 M. It is apparent that the performance of the passive cell is limited by the slow mass transport of formic acid at the low formic acid concentration range. As formic acid concentration is increased from 3 to 10 M, its concentration gradient is also increased between the anode fuel reservoir and the anode catalyst layer. Hence, the mass transport of formic acid in the anode as well as the overall passive cell performance is improved as formic acid concentration is increased from 3 to 10 M.

In our previous study on the Pd based active DFAFC, the catalytic activity of the Pd black is decreased as formic acid concentration is increased from 3 to 20 M [8]. Similar to the active DFAFC, the passive DFAFC shows a decrease in the catalytic activity of the Pd black as formic acid concentration is increased from 10 to 15 M in Fig. 7. According to Fig. 7, as formic acid concentration is increased from 10 to 15 M, the overall anode potential increases. This increase in the anode potential clearly indicates that the catalytic activity of the Pd black in the passive DFAFC decreases as formic acid concentration is increased. Additionally, our previous study indicates that the formic acid crossover flux also increases as the formic acid concentration is increased from 3 to 15 M. This fuel crossover flux creates so called "a mixed potential" at the cathode and decreases the overall cell performance. Thus, both the decreasing activity of the Pd black anode catalyst and the increasing fuel crossover flux are two of main reasons to account for the performance drop that we seen in Figs. 5 and 6 at the high formic acid concentration range.

As the formic acid concentration is increased, there are both positive and negative effects: increasing the fuel (formic acid) transport rate is the positive effect, while both the decreasing the Pd black's catalytic activity and the increasing the fuel crossover flux are the negative effects. At 10 M formic acid, the fuel transport is no longer a major limiting factor. If formic acid concentration is increased beyond 10 M and becomes too high, the performance losses from both the low anode catalytic activity seen in Fig. 7 and the fuel crossover flux dominate over the performance gain from the improved fuel transport rate. Hence, the overall cell performance decreases as formic acid concentration is increased from 10 to 15 M.

Previous study by Rice and Rhee speculated that concentrated formic acid solutions dehydrate a thin layer near the surface of a Nafion® membrane [4,12]. The dehydrated Nafion® membrane would decrease the proton conductivity and increase the cell resistance; hence, it would decrease the overall cell performance [4]. According to Fig. 8, the resistance of the passive DFAFC is relatively constant at formic acid concentration between 3 and 15 M. This indicates that the membrane dehydration effect is not a major issue for the passive DFAFC with formic acid concentration at 15 M and below.

Figs. 9 and 10 show that our passive DFAFC runs successfully at 0.72 V (with the constant voltage mode) or 100 mA cm^{-2} (with the constant current mode) for a reasonable time. According to Fig. 10, after 3 h of the run time, the performance of the passive cell is decreased dramatically while the anode over-potential increases rapidly. However, the cathode potential is relatively stable over 10 h in Fig. 10. Based on Fig. 10, it is apparent that the increase of the anode over-potential is a main reason for having a poor cell performance after operating it for 3 h. The fuel depletion causes this increase of the anode over-potential. As the fuel is consumed by the oxidation reaction and evaporated to the atmosphere over the operation time, there is less fuel available for the anode catalyst layer to react. This fuel depletion is clearly evidenced by Fig. 10. As the passive cell is refueled with the fresh 10 M formic acid at 4.4 and 7.3 h (265 and 440 min), the anode over-potential is decreased rapidly and the passive cell restores back most of its original performance.

5. Conclusion

The Pd based passive air breathing DFAFC was constructed and its performances were tested. The results in this paper show that our passive DFAFC is a good alternative power source, which can replace the conventional battery for small electronic devices in the future. Our passive DFAFC can be operated at a much higher fuel concentration range than a typical DMFC. Our passive DFAFC, at 10 M formic acid, produced the power density of 177 mW cm^{-2} at 0.53 V. The performance of the passive DFAFC decreased as the formic acid concentration was increased from 10 to 15. Both the decreasing of the anode catalytic activity and the increasing of the fuel crossover flux were two of main reasons for having the low cell performance at the high concentration of formic acid range. Despite this increase of the anode potential at the high formic acid concentration range, our passive cell at 15 M formic acid still produced the maximum power density of 147 mW cm^{-2} at 0.53 V, which is about the best power density value reported for the passive DMFC in literature at a much lower fuel concentration and higher operating temperature. Dehydration of the membrane at high formic acid concentration range is not a major issue for our passive DFAFC, as seen by the stable cell resistance in Fig. 8.

Acknowledgements

This material is based upon work supported by the Defense Advanced Research Projects Agency under U.S. Air Force grant F33615-01-C-2172 and by the U.S. Department of Energy under grant DEGF-02-99ER14993. Any opinions, findings, and conclusions or recommendations expressed in this publication are those of the authors and do not necessarily reflect the views of the U.S. Air Force, The Department of Energy or the Defense Advanced Research Projects Agency.

References

[1] B.J. Feder, New York Times, New York, 2003.
[2] A. Blum, et al., J. Power Sources 117 (2003) 22–25.
[3] H. Chang, et al., Solid State Ionics 148 (2002) 610.
[4] C. Rice, et al., Direct formic acid fuel cells, J. Power Sources 111 (1) (2002) 83–89.
[5] C. Rice, et al., Catalysts for direct formic acid fuel cells, J. Power Sources 115 (2) (2003) 229–235.
[6] S. Ha, B. Adams, R.I. Masel, A miniature air breathing direct formic acid fuel cells, J. Power Sources 128 (2) (2004) 119–124.
[7] Y. Zhu, S. Ha, R.I. Masel, High power density direct formic acid fuel cells, J. Power Sources 130 (1–2) (2004) 8–14.
[8] S. Ha, et al., Direct formic acid fuel cells with 600 A cm^{-2} at 0.4 V and 22 C, Fuel Cells 4 (4) (2004) 337–343.
[9] J. Larminie, A. Dicks, Fuel Cell Systems Explained, John Wiley & Sons, New York, 2000.
[10] J.G. Liu, et al., The effect of methanol concentration on the performance of a passive DMFC, Electrochem. Commun. 7 (2005) 288–294.
[11] D. Kim, et al., Recent progress in passive direct methanol fuel cells at KIST, J. Power Sources 130 (2003) 172–177.
[12] Y.W. Rhee, S.Y. Ha, R.I. Masel, Crossover of formic acid through Nafion® membranes, J. Power Sources 117 (1–2) (2003) 35–38.